J|A|C|S ARTICLES

Published on Web 10/19/2009

Comprehensive Investigation of the Energetics of Pyrimidine Nucleoside Formation in a Model Prebiotic Reaction

Yinghong Sheng,*,† Heather D. Bean,‡ Irena Mamajanov,‡ Nicholas V. Hud,‡ and Jerzy Leszczynski*,§

Department of Chemistry and Mathematics & Whitaker Center, College of Arts & Sciences, Florida Gulf Coast University, 10501 FGCU Boulevard South, Fort Myers, Florida 33965, School of Chemistry and Biochemistry, Georgia Institute of Technology, 901 Atlantic Drive, Atlanta, Georgia 30332, and Interdisciplinary Nanotoxicity Center, Department of Chemistry, Jackson State University, P.O. Box 17910, 1400 J. R. Lynch Street, Jackson, Mississippi 39217

Received February 2, 2009; E-mail: ysheng@fgcu.edu; jerzy@ccmsi.us

Abstract: The problem of β-nucleoside formation under prebiotic conditions represents one of the most significant challenges to the "RNA world" hypothesis. The possibility exists that alternative bases may have come before the contemporary bases (i.e., A, G, C, and U), including bases that more readily form nucleosides. We previously reported the first successful synthesis of a pyrimidine nucleoside from a free base and a nonactivated sugar in a plausible prebiotic reaction. Here we present a detailed computational study on the reaction at the density functional theory (DFT) level. The catalytic role of a Mg^{2+} ion on the reaction mechanism is also investigated. Our calculations demonstrate that a Mg^{2+} ion, serving as a Lewis acid, can afford the necessary stabilization to the base and leaving water molecule during glycoside bond formation. The solvent effect is considered by the Onsager solvation model and also by an extended model with the addition of explicit water molecules within the SCRF solvation model. In addition, predictions regarding the formation of nucleosides from other pyrimidine bases are also addressed, providing valuable insights into what chemical features of the bases facilitate glycoside formation in drying−heating reactions.

I. Introduction

The formation of a glycosidic bond between ribose and free pyrimidine bases under plausible prebiotic conditions has represented a serious challenge to the "RNA world" hypothesis and also to a number of its proposed precursors.[1] Over 30 years ago, Orgel and co-workers demonstrated that adenine and hypoxanthine form glycosidic bonds with D-ribose when dried and heated together.[2] However, this simple approach proved to be less promising with the other bases: neither cytosine nor uracil give rise to nucleosides under these conditions, nor does guanine, which may be due to the low solubility of the free guanine base.[1]

Some research groups have elected to explore completely different pathways to prebiotic pyrimidine nucleoside formation, including the construction of the cytosine base on a sugar phosphate. A stepwise synthesis of the base cytosine on a preformed sugar was first accomplished by Sanchez and Orgel,[3] and more recently explored in greater detail by the Sutherland laboratory.[4] This approach has proven to be regioselective, yielding very little β-cytidine. The α-cytosine ribonucleoside can be photoisomerized to the β-ribonucleoside, but in low yield. Improvements in β-cytidine formation by this approach are possible with phosphorylated ribose precursors or in a phosphate-rich reaction medium,[5,6] but the prebiotic relevance of phosphorylated compounds presents another difficulty and it is therefore important to seek alternative solutions to this problem.[7]

For the model prebiotic reactions discussed above, none of these approaches is able to produce all four nucleosides, or even one purine and one pyrimidine. If the original bases differed from the canonical AUCG,[8] then there is the possibility that some of these bases might have formed glycosides more easily than the current bases under prebiotic conditions. As part of our investigation of this hypothesis, we recently reported the first successful synthesis of a pyrimidine nucleoside from a free base (2-pyrimidinone) and a nonactivated sugar (D-ribose) in a plausible prebiotic reaction.[9] However, it is still not clear what causes a kinetic barrier to the glycosidic bond formation for the pyrimidines uracil and cytosine, and until a reasonably efficient and plausibly prebiotic synthesis is found for uridine and cytidine, it will be difficult to accept the proposal that RNA was the first informational polymer of life.

Given the fundamental importance of the glycosidic bond to many aspects of chemistry and biology, the theoretical study on glycosidic bond formation has received surprisingly little attention. Most theoretical studies have focused on glycosidic

† Florida Gulf Coast University.
‡ Georgia Institute of Technology.
§ Jackson State University.

(1) Zubay, G.; Mui, T. *Origins Life Evol. B.* **2001**, *31*, 87.
(2) Fuller, W. D.; Sanchez, R. A.; Orgel, L. E. *J. Mol. Evol.* **1972**, *1*, 249.
(3) Sanchez, R. A.; Orgel, L. E. *J. Mol. Biol.* **1970**, *47*, 531.
(4) Ingar, A.-A.; Luke, R. W. A.; Hayter, B. R.; Sutherland, J. D. *ChemBioChem* **2003**, *4*, 504.
(5) Powner, M. W.; Anastasi, C.; Crowe, M. A.; Parkes, A. L.; Raftery, J.; Sutherland, J. D. *ChemBioChem* **2007**, *8*, 1170.
(6) Powner, M. W.; Gerland, B.; Sutherland, J. D. *Nature* **2009**, *459*, 239.
(7) Keefe, A. D.; Miller, S. L. *J. Mol. Evol.* **1995**, *41*, 693.

10.1021/ja900807m CCC: $40.75

bond solvolysis.[10−13] Stubbs and Marx presented a Car−Parrinello molecular dynamics study on the mechanism of acid-catalyzed glycosidic bond formation between methanol and α-D-glucopyranoside in aqueous solution at 300 K.[14] Due to the differences in the reactants and reaction conditions, the reaction mechanism for pyrimidine nucleoside formation is expected to be different. Therefore, a comprehensive theoretical study is desirable. In this work, we present a detailed computational study of glycosidic bond formation during a pyrimidine nucleoside formation reaction at the density functional theory (DFT) and the MP2 level of theory. The goal of this study is (1) to determine the mechanistic details of the glycosidic bond formation in a pyrimidine nucleoside from a free base and a nonactivated sugar in a plausible prebiotic reaction, (2) to provide insights regarding optimal prebiotic reaction conditions for nucleoside formation, (3) to investigate the role of metal ions in the reaction mechanism, (4) to study the solvent effect on the reaction mechanism, as well as (5) to explore different pyrimidine base analogues that would be able to form the glycosidic bond under reaction conditions that have been demonstrated for purine and 2-pyrimidinone nucleoside synthesis.

II. Computational and Experimental Methodologies

A. Computational Methodologies. The choice of theoretical level for a given chemical problem depends on the required accuracy and the size of a molecule. DFT-B3LYP method has been demonstrated to predict excellent molecular geometries.[15] Therefore, the possible reaction mechanisms for the glycosidic bond formation between ribose and the free nucleoside bases (2-pyrimidinone, an analogue of uracil and cytosine) were studied using the B3LYP nonlocal density functional approximation.[16] In order to address what causes the kinetic barrier to glycosidic bond formation for pyrimidines, the reaction between ribose and uracil was also studied for comparison. The geometry of reactants, products, transition states, and intermediates were optimized by means of the Berny approach, a modified Schlegel method.[17] Vibrational frequency calculations were performed to confirm whether the obtained geometry represents a transition or minimum energy structure.

The 6-31G(d) basis set is a good compromise between efficiency and accuracy[18] and has been proven to reproduce molecular parameters well. The further expansion of the basis set has less impact on the accuracy of the molecular geometries.[19] We have also used the 6-311+G(d,p) and 6-31++G(d,p) basis sets for some of the studied species and obtained similar geometrical parameters as predicted with the smaller basis set. In addition, the energy evaluations for the Mg^{2+}-catalyzed reaction at the B3LYP/6-311+G(d,p), B3LYP/6-31++G(d,p), and MP2/6-311++G(d,p) levels do not alter the reaction mechanism. Therefore, we will report the results obtained from the 6-31G(d) basis set unless otherwise noted.

The reactions, to which the theoretical models are compared, were conducted in dH_2O solutions. The solvent effects on the reaction mechanism were first studied by using the Onsager model.[20] In this model, the liquid is represented by a dielectric continuum, characterized by its dielectric constant, ε. The solute is placed in a cavity created in the continuum. The distribution of electronic density of the solute polarizes the continuum and generates an electric field inside the cavity, which in turn affects the geometry and electronic structure. In order to mimic the experimental conditions, the dielectric constant of $\varepsilon = 78.39$ (corresponding to water) was used.

However, the specific interactions, such as hydrogen bonding, are not included in the Onsager model. In the literature, different approaches have been adopted in order to study the effect of bulk water on the reaction mechanisms. Car−Parrinello ab initio molecular dynamics[14,21] would be an excellent tool to study the role of water molecules, especially when water molecules are directly involved in the proton-transfer process. The combined hybrid SCRF solvation models with explicit water molecules have also been shown to be successful.[22] In this work, we investigated the role of specific water molecules using the Onsager solvation model with explicit water molecules in the second coordination sphere or shell[23] of the complexes. All explicit molecule conformations were optimized. All calculations were carried out using the Gaussian 03 program.[24]

B. Materials and Experimental Methods. Zebularine and 2-pyrimidinone were obtained from Sigma-Aldrich. Magnesium chloride was dried in vacuo prior to use. For solution-state studies of zebularine glycosidic bond cleavage, 200 μL portions of solutions containing 48 mM zebularine with and without 3.6 M $MgCl_2$ were

(8) (a) Benner, S.; Burgstaller, P.; Battersby, T.; Jurczyk, S. Did the RNA world exploit an expanded genetic alphabet? In *The RNA World. Second Edition: The Nature of Modern RNA Suggests a Prebiotic RNA World*; Gesteland, R. F., Atkins, J. F., Eds.; Cold Spring Harbor Laboratory Press: Cold Spring Harbor, NY, 1999; pp 163−181. (b) Hud, N. V.; Anet, F. A. L. *J. Theor. Biol.* **2000**, *205*, 543. (c) Kolb, V. M.; Dworkin, J. P.; Miller, S. L. *J. Mol. Evol.* **1994**, *38*, 549. (d) Mittapalli, G. K.; Osornio, Y. M.; Guerrero, M. A.; Reddy, K. R.; Krishnamurthy, R.; Eschenmoser, A. *Angew. Chem., Int. Ed.* **2007**, *46*, 2478. (e) Mittapalli, G. K.; Reddy, K. R.; Xiong, H.; Munoz, O.; Han, B.; De Riccardis, F.; Krishnamurthy, R.; Eschenmoser, A. *Angew. Chem., Int. Ed.* **2007**, *46*, 2470.

(9) Bean, H. D.; Sheng, Y.; Collins, J. P.; Leszczynski, J.; Hud, N. V. *J. Am. Chem. Soc.* **2007**, *129*, 9556.

(10) Fothergill, M.; Goodman, M. F.; Petruska, J.; Warshel, A. *J. Am. Chem. Soc.* **1995**, *117*, 11619.

(11) Dinner, A. R.; Blackburn, G. M.; Karplus, M. *Nature* **2001**, *413*, 752.

(12) Gu, J.; Xie, Y.; Schaefer III, H. F. *J. Am. Chem. Soc.* **2005**, *127*, 1053.

(13) Torres, R. A.; Himo, F.; Bruice, T. C.; Noodleman, L.; Lovell, T. *J. Am. Chem. Soc.* **2003**, *125*, 9861.

(14) (a) Stubbs, J. M.; Marx, D. *Chem.—Eur. J.* **2005**, *11*, 2651. (b) Stubbs, J. M.; Marx, D. *J. Am. Chem. Soc.* **2003**, *125*, 10960.

(15) (a) Bauschlicher, C. W. *Chem. Phys. Lett.* **1995**, *246*, 40. (b) El-Azhary, A. A.; Suter, H. U. *J. Phys. Chem.* **1996**, *100*, 15056.

(16) (a) Lee, C.; Yang, W.; Parr, R. *Phys. Rev. B.* **1988**, *37*, 785. (b) Becke, A. D. *J. Chem. Phys.* **1993**, *98*, 5648. (c) Miehlich, B.; Savin, A.; Stoll, H.; Preuss, H. *Chem. Phys. Lett.* **1989**, *90*, 5622. (d) Stephens, P. J.; Devlin, F. J.; Chabalowski, C. F.; Frisch, M. J. *J. Phys. Chem.* **1994**, *98*, 11623.

(17) Schlegel, H. B. *J. Comput. Chem.* **1982**, *3*, 214.

(18) (a) Sheng, Y.; Leszczynski, J.; Garcia, A. A.; Rosario, R.; Gust, D.; Springer, J. *J. Phys. Chem. B* **2004**, *108*, 16233. (b) Holmén, A.; Broo, A. *Int. J. Quantum Chem.* **1995**, *QBS22*, 113. (c) Broo, A.; Holmén, A. *Chem. Phys.* **1996**, *211*, 147.

(19) (a) Hariharan, P. C.; Pople, J. A. *Chem. Phys. Lett.* **1972**, *66*, 217. (b) Hehre, W. J.; Radom, L.; Schleyer, P. v. R.; Pople, J. A. *Ab Initio Molecular Orbital Theory*; Wiley: New York, 1986.

(20) (a) Cossi, M.; Scalmani, G.; Rega, N.; Barone, V. *J. Chem. Phys.* **2002**, *117*, 43. (b) Cances, M. T.; Mennucci, V.; Tomasi, J. *J. Chem. Phys.* **1997**, *107*, 3032. (c) Onsager, L. *J. Am. Chem. Soc.* **1936**, *58*, 1486. (d) Kirkwood, J. G. *J. Chem. Phys.* **1934**, *2*, 351. (e) Wong, M. W.; Frisch, M. J.; Wiberg, K. B. *J. Am. Chem. Soc.* **1991**, *113*, 4776. (f) Wong, M. W.; Wiberg, K. B.; Frisch, M. J. *J. Am. Chem. Soc.* **1992**, *114*, 523. (g) Wong, M. W.; Wiberg, K. B.; Frisch, M. J. *J. Chem. Phys.* **1991**, *95*, 8991. (h) Wong, M. W.; Wiberg, K. B.; Frisch, M. J. *J. Am. Chem. Soc.* **1992**, *114*, 1645.

(21) (a) Car, R.; Parrinello, M. *Phys. Rev. Lett.* **1985**, *55*, 2471. (b) Marx, D.; Hutter, J. *Ab-initio Molecular Dynamics: Theory and Implementation*; Modern Methods and Algorithms in Quantum Chemistry Forschungzentrum Juelich, NIC Series; 2000; Vol. 1, http://www.theochem.ruhr-uni-bochum.de/research/marx/cprev.en.html.

(22) (a) Privalo, T.; Samec, J. S. M.; Bckvall, J.-E. *Organometallics* **2007**, *26*, 2840. (b) Cimino, P.; Barone, V. *THEOCHEM* **2005**, *729*, 1. (c) Amovilli, C.; Barone, V.; Commi, R.; Cances, E.; Cossi, M.; Mennucci, B.; Pomelli, C. S.; Tomasi, J. *Adv. Quantum Chem.* **1999**, *32*, 227. (d) Brancato, G.; Di Nola, A.; Barone, V.; Amadei, A. *J. Chem. Phys.* **2005**, *122*, 154109.

(23) Sheng, Y.; Roszak, S.; Leszczynski, J. *J. Chem. Phys.* **2004**, *120*, 4324.

(24) Frisch, M. J.; et al. *Gaussian 03,* Revision E.01; Gaussian, Inc., Wallingford CT, 2004.

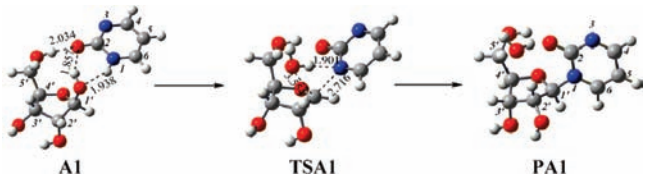

Figure 1. A possible reaction pathway between ribose and 2-pyrimidinone in the gas phase. Labeled distances are in angstroms. The structures are depicted using standard CPK coloration.

incubated in individual vials at 100 °C. Vials were removed at designated times and stored at 4 °C until analyzed by HPLC. A saturated solution of $MgCl_2$ (calculated to be 4.8 M at 100 °C) containing 48 mM zebularine was stirred at 100 °C, with 200 μL aliquots removed every hour and stored at 4 °C until analyzed.

For drying−heating measurements of zebularine glycosidic bond cleavage, 200 μL portions of solutions containing 5 mM zebularine and 200 mM $MgCl_2$ were dried for periods of 15−120 min at 100 °C on 2 in. watch glasses. Each watch glass was then washed three times with 200 μL of deionized water, and washings were combined and lyophilized. The solid was resuspended in 200 μL of water prior to HPLC analysis.

For all samples, HPLC separation was conducted using a Phenomenex Luna NH_2 column (4.6 × 250 mm, 5 μ) and 80% acetonitrile:20% water isocratic elution at 1 mL/min flow rate. Zebularine degradation was determined by comparing the integrated HPLC peak intensity of free 2-pyrimidinone with the intensity of the remaining zebularine.

III. Results and Discussion

A. Reaction of Ribose with 2-Pyrimidinone and Uracil without Mg^{2+}. Several possible mechanisms for the reaction between ribose and 2-pyrimidinone have been investigated. At the initiation of our theoretical studies, we had hypothesized that the hydroxypyrimidine tautomer of 2-pyrimidinone might be the tautomer active during glycosidic bond formation. However, our calculations revealed that the keto−enol tautomerisms of 2-pyrimidinone or protonated 2-pyrimidinone are hampered by high activation energies (see Figure S1 of Supporting Information). Therefore, it is unlikely that the formation of β-nucleoside takes place through the hydroxypyrimidine tautomer, but rather through the pyrimidinone tautomer, which is the preferred tautomer of 2-pyrimidnone in aqueous solution. Stubbs and Marx[14] also proposed that the formation of methyl β-glucopyranoside from α-D-glucopyranose and methanol proceeded through a D_NA_N mechanism, which involves the formation of oxocarbenium ion. In our experiment,[9] only the β-conformation of the furanosyl ribonucleosides was observed from the condensation of 2-pyrimidinone with D-ribose; no α-furanosyl ribonucleoside was observed and, if present, formed only in low yields. Therefore, the formation of the C−N glycosidic bond in β-furanosyl ribonucleoside does not follow the D_NA_N mechanism. Under this circumstance, we recognize that holding 2-pyrimidinone and the ribose C1′ hydroxyl in close proximity is crucial to form only the β-furanosyl ribonucleoside.

We first studied two possible reaction mechanisms of glycosidic bond formation between ribose and 2-pyrimidinone in the gas phase by holding 2-pyrimidinone and the ribose C1′ hydroxyl in close proximity. For comparison, the analogous reaction between ribose and uracil was also investigated.

Reaction between Ribose and 2-Pyrimidinone without Mg^{2+}. Figure 1 shows a possible reaction pathway for the glycosidic bond formation between ribose and 2-pyrimidinone.

Table 1. B3LYP/6-31G(d)-Predicted Activation Energies of Glycosidic Bond Formations between Ribose and 2-Pyrimidinone, Uracil (in kcal/mol)

	pathway A	pathway B
Gas Phase		
ribose + pyrimidinone	52.7[a]	61.1
ribose + uracil	50.8[a]	59.2
ribose + protonated-pyrimidinone	−	34.3
Water		
ribose + pyrimidinone	49.4	52.2
ribose + uracil	46.6	51.4
With Mg^{2+}		
ribose + protonated pyrimidinone + Mg^{2+}	20.2[a,b,c]	
ribose + uracil + Mg^{2+}	39.9[a]	−

[a] Data were originally reported in ref 9. [b] $\Delta E^{\ddagger} = 25.44$ kcal/mol, the single-point relative energies in water at the B3LYP/6-31G(d)-SCRF (Onsager solvation model) optimized geometries. [c] $\Delta E^{\ddagger} = 25.20$ kcal/mol, at extended model with the addition of explicit water molecules within the SCRF solvation model; all explicit molecule conformations were optimized.

In this reaction pathway, 2-pyrimidinone first forms a complex (**A1**) with ribose. The complex is stabilized by three hydrogen-bonding interactions: one between the ribose C1′ hydroxyl oxygen atom (O1′) and the N1 proton (H1) of 2-pyrimidinone, the second between the 2-pyrimidinone carboxyl oxygen atom and the O1′ proton of ribose, and the third between the C5′ hydroxyl (O5′) proton of ribose and the carboxyl oxygen of 2-pyrimidinone. The corresponding hydrogen-bond distances amount to 1.938, 1.857, and 2.034 Å, respectively.

In the **A1** complex, the orientation of 2-pyrimidinone with respect to ribose, with H1 pointing toward O1′, facilitates the proton transfer from N1 to O1′. As H1 approaches O1′, the C1′−O1′ bond breaks. At the same time N1 of 2-pyrimidinone approaches C1′ of ribose. A transition state corresponding to the transfer of H1 from N1 to O1′ and the cleavage of the C1′−O1′ bond, as well as the formation of C1′−N1 bond (**TSA1**) was identified and is shown in Figure 1. In the transition structure **TSA1**, the distance between C1′ and O1′ elongates to 3.554 Å, indicating that the C1′−O1′ bond is broken at this point. The leaving OH group captures H1 and forms a water molecule in **TSA1**. The distance between N1 and C1′ amounts to 2.716 Å. The activation energy for this pathway is calculated to be 52.7 kcal/mol.

2-Pyrimidinone can also approach ribose in a different orientation where the carboxyl group is closer to the C3′ hydroxyl group (see Figure S2, Supporting Information), and similarly, a high activation energy is predicted (61.13 kcal/mol). The relative energies of the nucleoside product, zebularine, from both pathways (**PA1** and **PB1**) are −8.00 and −0.43 kcal/mol, respectively, at the B3LYP/6-31G(d) level, indicating that both pathways are exothermic and thermodynamically feasible. However, the high activation energies for both pathways reveal that glycosidic bond formation between ribose and 2-pyrimidinone in the gas phase is kinetically inaccessible. In addition, the activation energies for both pathways in water were also evaluated by the Onsager solvation model and it was found that the solvent effect only slightly lowers the activation barriers (see Table 1). Therefore, the glycosidic bond formation between ribose and a free 2-pyrimidinone base would not likely take place in the gas phase or in pure water.

Reaction between Ribose and Uracil without Mg^{2+}. For comparison, the possible reaction mechanisms of the glycosidic bond formation between ribose and uracil were also studied.

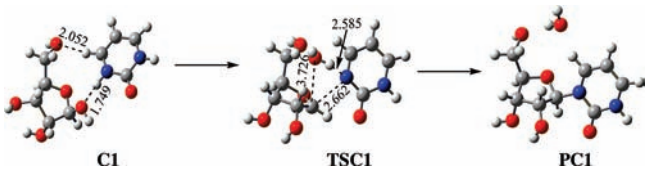

Figure 2. Acid-catalyzed glycosidic bond formation between ribose and 2-pyrimidinone in the absence of Mg^{2+}. Labeled distances are in angstroms. The structures are depicted using standard CPK coloration.

Two pathways similar to those of zebularine formation are shown in Figure S3 (Supporting Information). Both pathways possess high activation energies, 50.8 and 59.2 kcal/mol at the B3LYP/6-31G(d) level. The inclusion of solvent effect only slightly reduces the activation energies to 46.6 and 51.4 kcal/mol, respectively (Table 1). This indicates that it is also unlikely for uracil and ribose to form uridine in the gas phase or in a pure water solution.

B. Brønsted Acid Catalyzed Reaction between Ribose and 2-Pyrimidinone without Mg^{2+}. In our previous work,[9] β-ribonucleosides were synthesized from adenine (adenosine), hypoxanthine (inosine), and 2-pyrimidinone (zebularine) under two reaction conditions: at pH 2.1 in the presence of a Brønsted acid and at neutral pH in the presence of the Lewis acid, Mg^{2+}. Buffering the sample at pH 6.3 without the addition of magnesium salts reduced nucleoside production to an unobservable level, indicating that glycosidic bond formation is an acid-catalyzed reaction. As 2-pyrimidinone has a pK_a of 2.24,[25] the majority of the base will be protonated at pH 2.1, the acidic reaction condition created by the Brønsted acid; we therefore modeled glycosidic bond formation between protonated 2-pyrimidinone and ribose at the B3LYP/6-31G(d) level.

The acid-catalyzed reaction mechanism is shown in Figure 2. Only one pathway was located, similar to the uncatalyzed zebularine formation in the gas phase. Initially, the protonated 2-pyrimidinone forms a complex (**C1**) with ribose in which two H-bonds are found: one is between H1 of 2-pyrimidinone and O1′ of ribose, measuring 1.749 Å, and the other between the O5′ of ribose and H6 from 2-pyrimidinone, measuring 2.052 Å. Next, the C1′ and N1 approach each other, and H1 migrates from N1 of 2-pyrimidinone to the leaving C1′ hydroxyl group to form a free water molecule, corresponding to the transition structure (**TSC1**) shown in Figure 2. The distances between the C1′−N1, N1−H_{H_2O}, and C1′−O_{H_2O} amount to 2.662, 2.585, and 3.726 Å, respectively.

It is interesting that the distances between N1−H_{H_2O} and C1′−O_{H_2O} are elongated from 1.718 and 2.704 Å, respectively, in **TSB1** to 2.585 and 3.726 Å in **TSC1**, while the C1′−N1 distance shortens to 2.662 Å in **TSC1** from 2.915 Å in **TSB1**. These changes are due to charge redistribution when a proton is introduced into the system. The B3LYP/6-31G(d)-calculated charge densities are +2.052e for ribose and −0.548e for 2-pyrimidinone in **TSC1**, while the charge densities on ribose and 2-pyrimidinone in the uncatalyzed **TSB1** are +1.227e and −0.687e, respectively. The larger positive charge on the ribose fragment enhances the attraction between the ribose and the 2-pyrimidinone in the **TSC1**, which leads to a shorter C1′−N1 distance, and a dramatic decrease of the activation energy. The activation energy decreases from 61.1 kcal/mol for the uncatalyzed reaction in the gas phase to 34.3 kcal/mol for the acid-catalyzed reaction. These calculations help explain our experimental observations that zebularine formation is possible in the presence of a Brønsted acid.[9]

(25) Brown, D. J. *Nature* **1950**, *165*, 1010.

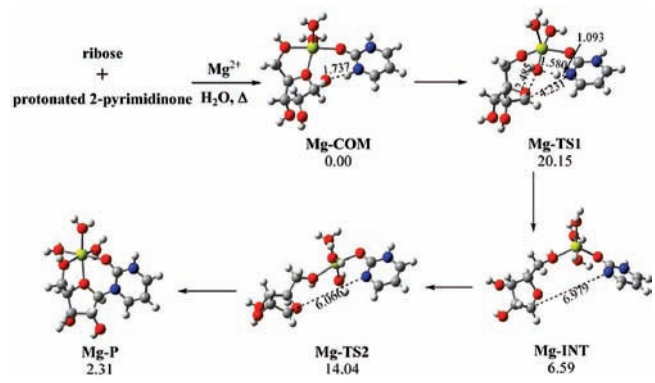

Figure 3. The structures and relative energies of reactants, complex, intermediate, transition structures, and product for the reaction between ribose and protonated 2-pyrimidinone in the presence of Mg^{2+}. Labeled distances are in angstroms. Magnesium is drawn in yellow, and all other atoms follow standard CPK coloration.

C. Lewis Acid Catalyzed Reaction of Ribose with 2-Pyrimidinone and Uracil in the Presence of Mg^{2+}. We have shown that zebularine formation by 2-pyrimidinone and ribose under drying conditions can be promoted by divalent metal ion salts at neutral pH,[9] as was shown in earlier investigations of purine nucleoside synthesis.[2] Among several divalent metal ions tested, Mg^{2+} is one of the most efficient catalysts for glycosidic bond formation (Hud laboratory, unpublished). We therefore studied glycosidic bond formation between protonated 2-pyrimidinone and ribose in the presence of the Lewis acid Mg^{2+} at the B3LYP/6-31G(d) level.

The mechanism for the reaction between protonated 2-pyrimidinone and ribose in the presence of Mg^{2+} (Figure 3) is found to be completely different from the mechanisms apparently favored in the absence of metal ions.

First, a distorted trigonal bipyramidal complex, **Mg-COM**, is formed between ribose and protonated 2-pyrimidinone with the assistance of a Mg^{2+} ion. The ribose is bidentately coordinated to the Mg^{2+} ion at O5′ and the ring oxygen, O4′. These coordinations are facilitated through the interactions of the lone pair electrons of the oxygen atoms and the d-orbitals of the Mg^{2+} ion. The other three vertices of the trigonal bipyramid are occupied by the protonated 2-pyrimidinone carboxyl oxygen atom and two water molecules. The ribose and the protonated 2-pyrimidinone are in cis-conformation so that the N1 proton of the protonated 2-pyrimidinone is orientated toward O1′, with a distance of only 1.737 Å. This orientation facilitates the transfer of the N1 proton to O1′.

In the **Mg-TS1** transition structure, the breaking of the C1′−O1′ bond is mediated by the Mg^{2+} ion. One can see from Figure 3 that a bond has actually formed between the leaving OH group and the Mg atom. It is also apparent that the Mg-bonded OH group forms a strong hydrogen bond with H1 of 2-pyrimidinone, with a bond length of only 1.580 Å. As a consequence, the N1−H1 bond elongates from 1.019 Å in **Mg-COM** to 1.093 Å in **Mg-TS1**. The presence of the Mg^{2+} ion greatly lowers the activation barrier needed to break the C1′−O1′ and N1−H1 bonds. The calculated activation energy amounts to 20.15 kcal/mol, which is much lower than the activation energies of the reaction mechanisms in the absence of a Mg^{2+} ion.

In the **Mg-TS1** transition structure the distance between C1′ and N1 measures 4.231 Å. It is expected that removing the

proton and hydroxyl group from 2-pyrimidinone and ribose, respectively, would clear the way for C1′ and N1 to form a glycosidic bond. However, instead of forming a zebularine product, the transition structure **Mg-TS1** leads to an intermediate **Mg-INT**, in which the distance between C1′ and N1 becomes quite long (6.979 Å at the B3LYP/6-31G(d) level). A larger basis set was also used to confirm these structural parameters, and the C1′−N1 distance only shortens to 6.929 Å at the B3LYP/6-31++G(d,p) level. Considering that the reaction takes place in water, the solvent effect was investigated by using the Onsager model at the B3LYP/6-31G(d) level. These results indicate that the solvent effect only slightly shortens the C1′−N1 distance (6.537 Å) in the intermediate **Mg-INT**.

In the transition structure **Mg-TS1**, the charge distributions on N1, H1, O_{OH}, and C1′ atoms are −0.634e, 0.447e, −0.873e, and 0.564e, respectively. There is a competition of attractions between both N1···H1 and H1···O_{OH} pairs. The stronger attraction between H1···O_{OH} facilitates the migration of H1 to the Mg-bonded hydroxyl group, forming a water molecule (**Mg-INT**). The newly formed Mg-bonded water molecule forms a hydrogen bond with the deprotonated nitrogen atom in the intermediate **Mg-INT** (Figure 3), with charge distributions on N1 and H_{H_2O} atoms of −0.567e and 0.312e, respectively. The existence of this strong interaction temporarily stabilizes the intermediate.

In order to form a glycosidic bond between the C1′ and N1 atoms, the interaction between the N1 and H_{H_2O} atoms must be removed. This can be achieved by rotation of the Mg-bound water molecule or the 2-pyrimidinone ring. In searching for the corresponding transition state, structure **Mg-TS2** was located (Figure 3). In this structure, the dihedral angle ∠C2−O2−Mg−O_{H_2O} between the pyrimidinone ring and the newly formed water molecule with respect to the Mg atom measures −84.0°, and the dihedral angles between the pyrimidinone ring and the other two water molecules with respect to the Mg atom (C2−O2−Mg−O_{H_2O}) are 175.5° and −93.5°. For comparison, in **Mg-INT** the corresponding dihedral angles are −12.05°, 86.7°, and 175.2°, respectively. This difference indicates that the pyrimidinone ring and newly formed water molecule have rotated away from each other to form **Mg-TS2**. The frequency analysis shows only one imaginary frequency (25.6i cm^{-1}) corresponding to the rotation of the pyrimidinone ring around the Mg−O2 bond, associated with the rotation of the newly formed water molecule in the opposite direction.

The existence of **Mg-TS2** is quite reasonable because the formation of the C1′−N1 bond is hampered by the hydrogen-bond interaction revealed in **Mg-INT**, while the rotations of the water molecule and the pyrimidinone ring remove this interaction, clearing the way for N1 to approach the C1′ atom. Since rotations usually require little energy, this step only needs to overcome a small activation barrier of about 7.5 kcal/mol. In **Mg-TS2**, the C1′−N1 distance amounts to 6.066 Å at the B3LYP/6-31G(d) level. An IRC analysis confirmed that the transition structure **Mg-TS2** is the transition state connecting the intermediate (**Mg-INT**) and the nucleoside product (**Mg-P**), a distorted octahedral complex.

The solvent effect on the reaction mechanism of zebularine formation was also investigated. The structures of the complex, reactants, transitions structures, and intermediate were reoptimized at the B3LYP/6-31G(d) level using the Onsager model. Table 2 summarizes the relative energies of all these species and the product of the Mg^{2+}-assisted reaction at the different levels of theory. We note that the energy profiles at the different levels of theory are similar. Thus, the use of a larger basis set and the inclusion of solvation effects do not change the reaction mechanism.

Table 2. Relative Energies, Activation Energies of Complexes, Transition Structures, Intermediates, and Product at the Different Levels of Theory (in kcal/mol)

	B3LYP/ 6-31G(d)[a]	B3LYP/ 6-31++G(d,p)[a]	MP2/ 6-31++G(d,p)[a]	B3LYP/ 6-31G(d)[b]
Mg-C1	0.00	0.00	0.00	0.00
Mg-TS1	20.15	19.00	22.89	25.44
Mg-INT	6.59	4.08	10.00	16.19
Mg-TS2	14.04	12.13	18.97	24.69
Mg-P	2.32	1.41	−5.31	9.31

[a] The single-point relative energies in the gas phase at the B3LYP/6-31G(d)-optimized geometries. [b] The single-point relative energies in water at the B3LYP/6-31G(d)-SCRF (Onsager solvation model) optimized geometries.

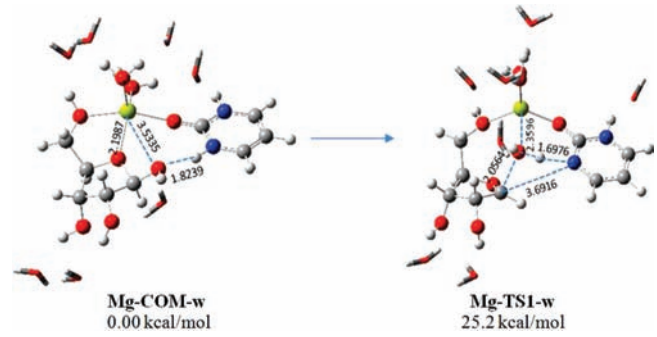

Figure 4. The optimized complex (**Mg-COM-w**) and transition state (**Mg-TS1-w**) of the rate-determining step of glycosidic C−N bond formation, at the B3LYP/6-31G(d) level using the SCRF solvation model with explicit water molecules. Labeled distances are in angstroms. Magnesium is drawn in yellow, and all other atoms follow standard CPK coloration.

The role of water molecules on the reaction mechanism in the presence of a Mg^{2+} ion was also investigated by an extended model with the addition of explicit water molecules within the SCRF solvation model. Only the first step of the reaction between ribose and 2-pyrimidinone was studied because it is the rate-determining step. The optimized structures of the complex (**Mg-COM-w**) and the transition state (**Mg-TS1-w**) are shown in Figure 4. From Figure 4 one can see that the additional water molecules only slightly change the geometrical parameters of the complex and the transition state, and the activation energy amounts to 25.2 kcal/mol. Such a small change in the activation energy is attributed to the fact that water molecules are not directly involved in the bond breaking and formation. Therefore, the results presented in our work, while somewhat limited due to the continuum solvent model, do provide a reasonable computational approach for comparing alternative possible reaction pathways and provide results that are consistent with experimental studies.

All levels of calculations demonstrate that the formation of the glycosidic bond between ribose and 2-pyrimidinone in the presence of a Mg^{2+} ion is a three-step reaction: First, 2-pyrimidinone is protonated in the acid solution and forms a complex with sugar with the assistance of a Mg^{2+} ion. Second, the C1′−O1′ bond breaks with the assistance of a metal atom, and the departing hydroxide group abstracts a proton from 2-pyrimidinone, yielding a water molecule. Finally, the rotations of the newly formed water molecule and the pyrimidinone ring clear the way for the creation of the glycosidic bond between the C1′ and N1 atom of 2-pyrimidinone so that the zebularine product is formed.

Figure 5. Pyrimidines tested in the nucleoside-formation reaction with ribose. (Bases are shown in their protonated forms.)

Reaction between Ribose and Uracil in the Presence of Mg^{2+}. For comparison, the optimized structures of the complex, transition structure, and product for the glycosidic bond formation between ribose and uracil in the presence of Mg^{2+} are shown in Figure S4 (Supporting Information). Unlike the reaction with 2-pyrimidinone, the reaction with uracil is a two-step reaction in the presence of Mg^{2+}: First the uracil forms a complex (**Mg-CU**) with ribose and then deprotonation of N1 of uracil and the breaking of the C1′−O1′ bond are asynchronically concerted with the glycosidic bond formation between atoms C1′ and N1. The predicted activation energy amounts to 39.9 kcal/mol in the gas phase. When the solvation effects are considered, the activation energy actually increases to 41.2 kcal/mol. Thus, the glycosidic formation between ribose and uracil is not likely to proceed under the reaction conditions investigated. These theoretical results are in agreement with our previous experimental observations[9] that 2-pyrimidinone forms β-nucleosides in good yield (greater yields than both adenine and hypoxanthine), while uracil does not form nucleosides in detectable yields under any of the conditions tested.

D. Will Other Pyrimidines Spontaneously Form Nucleosides with Ribose? The coupling of 2-pyrimidinone to ribose, as described in this work, can produce β-nucleosides in relatively good yield. However, the experimental conditions outlined above might be somewhat specific for glycosidic bond formation between 2-pyrimidinone and ribose. It remains to be demonstrated whether similar conditions favor nucleoside formation reactions with other pyrimidine bases and various sugars. Thus, it is of great interest to determine which chemical features of 2-pyrimidinone are essential for this reaction to occur. As a first step toward addressing this question, another pyrimidine related to 2-pyrimidinone was also tested for its ability to form nucleosides with ribose under similar reaction conditions. The structures of the three pyrimidines tested in this study are shown in Figure 5.

The pyrimidine most comparable to 2-pyrimidinone is 4-pyrimidinone. This base has exactly the same chemical composition as 2-pyrimidinone, but the carboxyl group at C4 is adjacent to only one nitrogen atom, rather than being in between the two nitrogen atoms of the pyrimidine ring. This structural difference is associated with the lower 4-pyrimidinone pK_a of 1.84, as compared the 2.24 pK_a of 2-pyrimidinone.[19] When free 4-pyrimidinone is heated and dried under mildly acidic conditions (pH 2.4) in the presence of ribose, products are observed with UV absorbance and HPLC retention times that are consistent with 4-pyrimidinone nucleoside formation (data not shown). However, these putative nucleosides are produced at most in one-fourth the yield of those formed in the analogous 2-pyrimidinone reaction (i.e., under similar reaction conditions). The decrease in the product yield in 4-pyrimidinone is potentially due to its lower pK_a, which results in a reduction of the protonated form of the base, relative to 2-pyrimidinone, at pH 2.4.

The details of the B3LYP/6-31G(d)-optimized structures of the pyrimidines are shown in Figure 5. Careful examination of the geometrical parameters of the 2-pyrimidinone and 4-pyrimidinone isomers reveals that the N−H bond length in the protonated 2-pyrimidinone amounts to 1.019 Å, 0.006 Å longer than in the unprotonated 2-pyrimidinone, which contributes to the lower energy required for the abstraction of the H1 proton during ribosylation. The N1−H1 and N3−H3 bond lengths in the protonated 4-pyrimidinone are 1.020 and 1.017 Å, respectively. It seems reasonable that the protons connected to either nitrogen atom of the pyrimidinone bases can be donated in the reaction. However, according to the transition structure **Mg-TS1** presented in the section III.C, the coordination of the carboxyl oxygen atom to the magnesium ion is crucial to maintain the orientation of the pyrimidine ring so that the proton can be transferred from the nitrogen atom to the hydroxyl group in the reaction pathway. Once coordinated, H1 of 4-pyrimidinone is simply too far away to be able to adopt a proper orientation with the C1′ hydroxyl group. We note, however, that a proton could alternatively be delivered from solution. Nevertheless, the N1−H1 bond would require more energy to break, as the bond length of N1−H1 is slightly shorter than the N3−H3 bond. ^{1}H and ^{1}H−^{13}C NMR data also indicate that N3 is more nucleophilic than N1, as the addition of 4-pyrimidinone to acetaldehyde (an open-chain model of an aldose sugar) occurs at N3 almost exclusively, i.e., no acetaldehyde addition at N1 was observed (see Figure S5 and Tables S1 and S2, Supporting Information). Combining these results, it is predicted that the nucleosides with 4-pyrimidinone connected through N3 to ribose would be more favored.

As discussed in the preceding section, the reaction of the uracil with ribose is apparently not favorable because of the localization of charge on N1, which enhances the N1−H1 bond strength (N−H bond lengths in uracil are short, being 1.011 and 1.014 Å) and creates a substantial kinetic barrier to pyrimidine glycosidic bond formation. The pK_a of N1 of uracil is about 9.5, so that there is less than 1% of the anionic form at neutral pH. However, Kimura et al.[26] have shown that placement of the uracil base near a cationic species can selectively reduce the pK_a of N1 by more than 2 pH units. Thus, coordination of uracil within a supramolecular assembly, such as in a coaxial stack with cationic intercalators,[8b] might sufficiently lower the N1 pK_a to allow glycosylation.

E. Nucleoside Degradation—Comparing Theory and Experiment. By the principle of microscopic reversibility, the transition state associated with glycosidic bond cleavage must be the same, under identical reaction conditions, as the transition state of glycosidic bond formation. The B3LYP/6-31G(d)-calculated activation energy for zebularine glycosidic bond cleavage, in water at neutral pH, is 26.1 kcal/mol. In the presence of Mg^{2+}, this activation energy is predicted to reduce to 13.6 kcal/mol. These calculations are consistent with the observation that the glycosidic bond of zebularine is much less stable than that of uridine,[9] which has calculated uncatalyzed and Mg^{2+}-catalyzed activation energies of 45.2 and 39.0 kcal/mol, respectively.

(26) Kimura, E.; Kitamura, H.; Koike, T.; Shiro, M. *J. Am. Chem. Soc.* **1997**, *119*, 10909.
(27) Burgess, J. *Metal Ions in Solution*; Ellis Horwood Ltd.: Chichester, England, 1978.

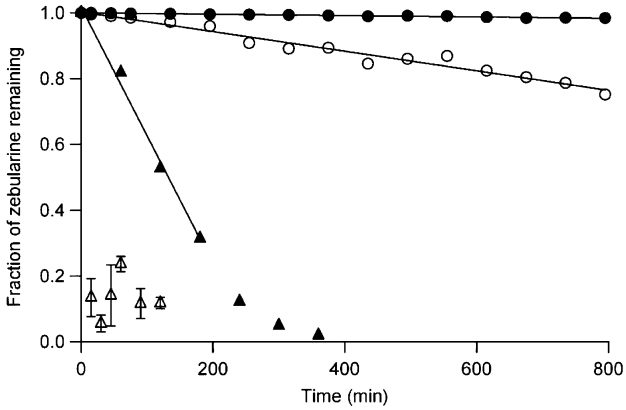

Figure 6. Hydrolysis of zebularine in the absence and presence of $MgCl_2$. Solution-state samples were 48 mM zebularine, in the absence of $MgCl_2$ (filled circles) and in the presence of 3.6 M $MgCl_2$ (open circles) and 4.8 M $MgCl_2$ (filled triangles). Zebularine samples dried and heated (open triangles) were initially 5 mM zebularine and 200 mM $MgCl_2$. All samples were neutral pH and maintained at 100 °C. Solid lines represent linear best fits of the initial rates of zebularine degradation for the solution-state samples. Error bars on dried and heated sample data represent the actual values obtained for duplicate experiments, for which the average is plotted. Calculated error bars for solution state data, based upon known sources of error, are comparable to the size of data markers.

The zebularine degradation reaction presents an opportunity to more directly compare theory and experiment, given that glycosidic bond cleavage is a first-order reaction. Specifically, we sought to compare experimental results for rates of zebularine glycosidic bond cleavage in the absence and presence of Mg^{2+} with the calculated change in transition barrier height corresponding to these reaction conditions. In Figure 6, the fraction of zebularine remaining (normalized to the total concentration of zebularine and free 2-pyrimidinone) is plotted as a function of time for four sets of nucleoside degradation reactions. All reactions were at 100 °C and neutral pH but differed in Mg^{2+} (and water) concentration/activity. In the absence of $MgCl_2$, the rate of zebularine degradation was measured to be 1.2×10^{-3} s^{-1}. In the presence of 3.6 M $MgCl_2$, this rate increases to 1.8×10^{-2} s^{-1} and in the presence of 4.8 M $MgCl_2$ to 0.23 s^{-1}. The increased rate of zebularine hydrolysis with increasing Mg^{2+} concentration and reduced water activity is consistent with Mg^{2+} acting as a catalyst in glycosidic bond cleavage. However, even at 4.8 M Mg^{2+}, the apparent reduction in the activation barrier to zebularine hydrolysis of 4 kcal/mol is below the predicted reduction of 12.5 kcal/mol. We note that 4.8 M Mg^{2+} corresponds to the saturation limit for $MgCl_2$ at 100 °C. Furthermore, Mg^{2+} in aqueous solution exists with a very favorable first shell of hydration.[27] Thus, to facilitate a more straightforward comparison with the calculated transition state that involves a partially dehydrated Mg^{2+} directly coordinated to zebularine, we also investigated the degradation of zebularine when dried from a solution containing $MgCl_2$ at 100 °C. For drying-heating times of 15−120 min, similar results were obtained. That is, an average of 13% of the zebularine remained after drying and heating, regardless of drying time. Thus, in 15 min or less, zebularine degradation was essentially complete, with the remaining zebularine apparently representing the equilibrium fraction of the nucleoside that exists during a step in the drying−heating process, i.e., where nucleoside formation and degradation are in equilibrium. Shorter drying times were not attempted due to uncertainty in the completeness and uniformity in sample drying, upon the basis of visual inspection of samples at shorter times (i.e., 5 min). Nevertheless, if we consider that 13% of the zebularine remains after 15 min, we are able to set a lower limit on the rate of zebularine degradation at 8.2 s^{-1}. Thus, drying in the presence of Mg^{2+} accelerates the rate of zebularine hydrolysis by greater than 6.5×10^3 over that measured in the absence of Mg^{2+}, corresponding to a decrease in transition barrier height of more than 6.6 kcal/mol, which is in the very least consistent with the predicted decrease of 12.5 kcal/mol. Given the apparent additional reduction in the barrier height of glycosidic bond cleavage upon drying from a solution containing $MgCl_2$, compared to that of a saturated $MgCl_2$ solution at the same temperature, our experimental results also support our computational models for Mg^{2+}-catalyzed glycosidic bond cleavage (and formation), which include direct nucleoside coordination of a partially dehydrated Mg^{2+} ion.

IV. Conclusions

The present work was motivated by the long-standing problem of how nucleosides were synthesized during the early stages of life. Although it has been known for decades that purine bases can form nucleosides with ribose when dried from an aqueous solution, albeit in low yield, the first plausible prebiotic synthesis of a pyrimidine nucleoside from a free base and a nonactivated sugar was reported only recently.[9] The lack of a mechanism for the prebiotic synthesis for the pyrimidine bases has been considered a crucial problem for most contemporary theories concerning the origin of life. The discovery that 2-pyrimidinone and other pyrimidine and pyrimidine-like bases can spontaneously form nucleosides with ribose has significant implications regarding the origin of the first RNA-like polymers, as it now seems feasible that both purine and pyrimidine nucleosides could have been formed on the prebiotic Earth without the aid of protein enzymes.

The reaction mechanisms of glycosidic bond formation between ribose and free 2-pyrimidinone base have been investigated by nonempirical theoretical calculations. The reaction potential energy surfaces of the studied reaction mechanisms are charted in Figure 7. Upon the basis of the results obtained, we can draw the following conclusions: (1) The theoretical study shows that the reaction between ribose and free 2-pyrimidinone would not likely take place in water at neutral pH due to the high activation energy. (2) The study of the reaction between ribose and protonated 2-pyrimidinone, which models an acidic experimental condition, shows that acid does catalyze glycosidic bond formation, as the activation energy decreases by 18.4 kcal/mol versus the reaction at neutral pH. (3) The formation of the β-ribofuranosyl nucleoside product is greatly facilitated by the presence of Mg^{2+} ions in the acidic solution (pH 2.1). Our theoretical investigation shows that the reaction between ribose and protonated 2-pyrimidinone in the presence of Mg^{2+} ions is a three-step reaction: First, 2-pyrimidinone is protonated in the acid solution and forms a complex with a ribose sugar with the assistance of a Mg^{2+} ion. Second, the C1′−O1′ bond breaks with the assistance of the metal ion, and the departing hydroxide group abstracts a proton from 2-pyrimidinone, yielding a water molecule. Finally, the rotations of the newly formed water molecule and the pyrimidinone ring clear the way for the formation of the glycosidic bond between the C1′ atom of ribose and N1 atom of 2-pyrimidinone. With the assistance of a Mg^{2+} ion at pH 2.1, the activation energy dramatically drops to 20.2 kcal/mol.

The activation energy of the zebularine formation reaction, at 20−25 kcal/mol in the presence of a Mg^{2+} ion, is consistent with the fact that the reaction requires only moderate heating at atmospheric pressure. The role of water molecules in the reaction mechanism was also investigated by the extended model with addition of explicit water molecules within the SCRF solvation model, but it was found to only slightly reduce the activation energy.

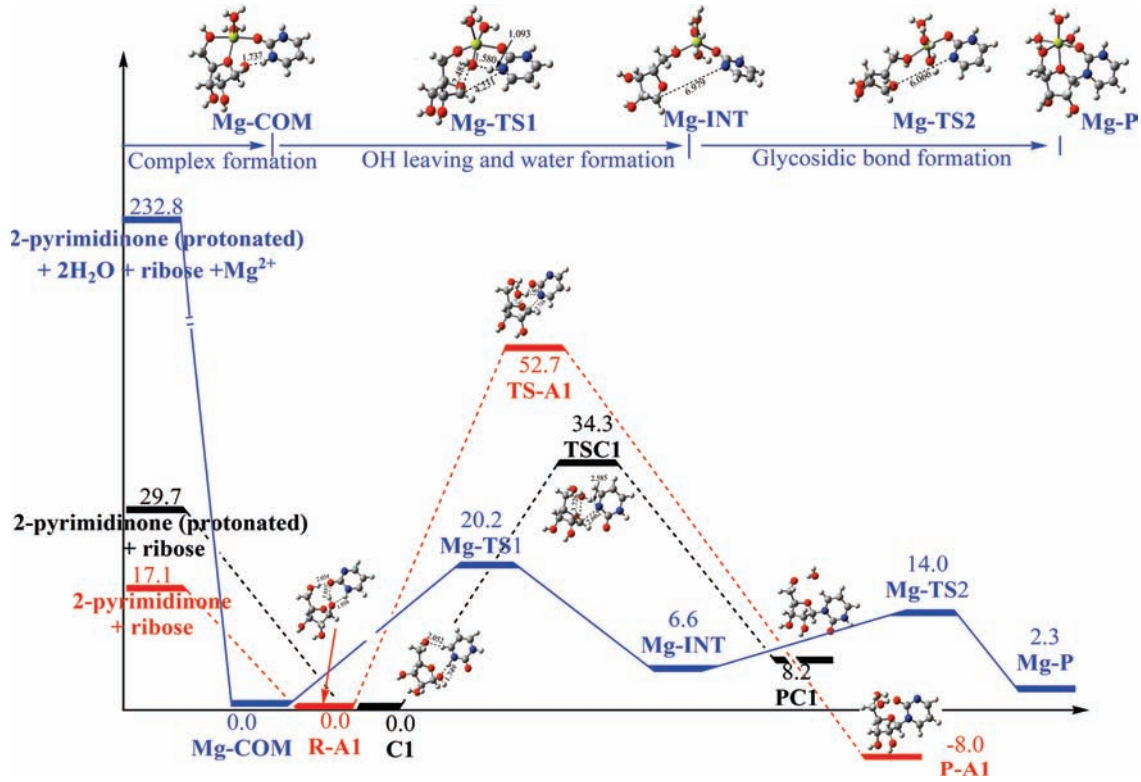

Figure 7. Potential energy surfaces for the zebularine formation reaction between 2-pyrimidinone and ribose (red) and between protonated 2-pyrimidinone and ribose (black) in the absence of Mg^{2+} and between protonated 2-pyrimidinone and ribose in the presence of Mg^{2+} (blue).

Important contributions to the study of prebiotic nucleoside formation have been made with phosphate/2′,3′-borate modifications of the sugar; therefore, it is of significant interest to understand these nucleoside formation reactions in the context of our proposed magnesium-mediated reaction mechanism.[28] Phosphate and borate are expected to affect the reactivity of ribose toward the bases due to the negative charges they carry. These studies are currently underway, and the comprehensive investigation on reaction mechanisms between 5′-phosphorylated ribose or 2′,3′-borate ribose and 2-pyrimidinone will be reported in a separate work.

Although the pyrimidine bases presently found in RNA do not spontaneously form nucleosides in a simple heating and drying reaction, our experimental observations[9] suggest that alternative pyrimidine (or pyrimidine-like) bases could have formed the nucleosides required for an ancestral RNA-like polymer. The protopyrimidine bases 2-pyrimidinone and 4-pyrimidinone studied in this work have more favorable glycosylation reaction kinetics than cytosine and uracil, suggesting that their nucleosides, or the nucleosides of other bases that more readily undergo glycosylation, could have been more abundant in the prebiotic environment and therefore might have been present in proto-RNAs. Within such a model for the origin of RNA, the proto-RNA nucleosides would have been originally selected for their more favorable chemistry of formation, but eventually replaced by uracil and cytosine through evolutionary processes based upon the superior nucleoside stability and functionality of these contemporary bases.

Acknowledgment. We thank A.E. Englehart for helpful discussions. This research was supported by the College of Arts & Sciences, Florida Gulf Coast University and National Science Foundation (Grant No. CHE-0739189).

Supporting Information Available: The keto−enol tautomerism transition structure and enol form of protonated 2-pyrimidinone (Figure S1); an alternative reaction pathway between ribose and 2-pyrimidinone in the gas phase (Figure S2); two possible reaction pathways between ribose and uracil in the gas phase (Figure S3); the structures of reactants, complex, intermediate, transition structures, and product for the reaction between ribose and uracil in the presence of Mg^{2+} (Figure S4); the ^{1}H NMR spectrum and the HSQC and HMBC $^{1}H-^{13}C$ correlational spectroscopy data of nucleophilic addition of 4-pyrimidinone to acetaldehyde (Figure S5, Tables S1 and S2); the full list of authors of ref 24; and Cartesian coordinates for all the stationary points optimized at the B3LYP/6-31G(d) level used in the paper (Table S3). This material is available free of charge via the Internet at http://pubs.acs.org.

JA900807M

(28) (a) Muller, D.; Pitsch, S.; Kittaka, A.; Wagner, E.; Wintner, C. E.; Eschenmoser, A. *Helv. Chim. Acta* **1990**, *73*, 1410–1468. (b) Ricardo, A.; Carrigan, M. A.; Olcott, A. N.; Benner, S. A. *Science* **2004**, *303*, 196. (c) Li, Q.; Ricardo, A.; Benner, S. A.; Winefordner, J. D.; Powell, D. H. *Anal. Chem.* **2005**, *77*, 4503. (d) Benner, S. A. *Acc. Chem. Res.* **2004**, *37*, 784. (e) Semmelhack, M. F.; Campagna, S. R.; Federle, M. J.; Bassler, B. L. *Org. Lett.* **2005**, *7*, 569.